Chapter 7
Controlling Factors in a Drug Delivery: Reverse Nucleation

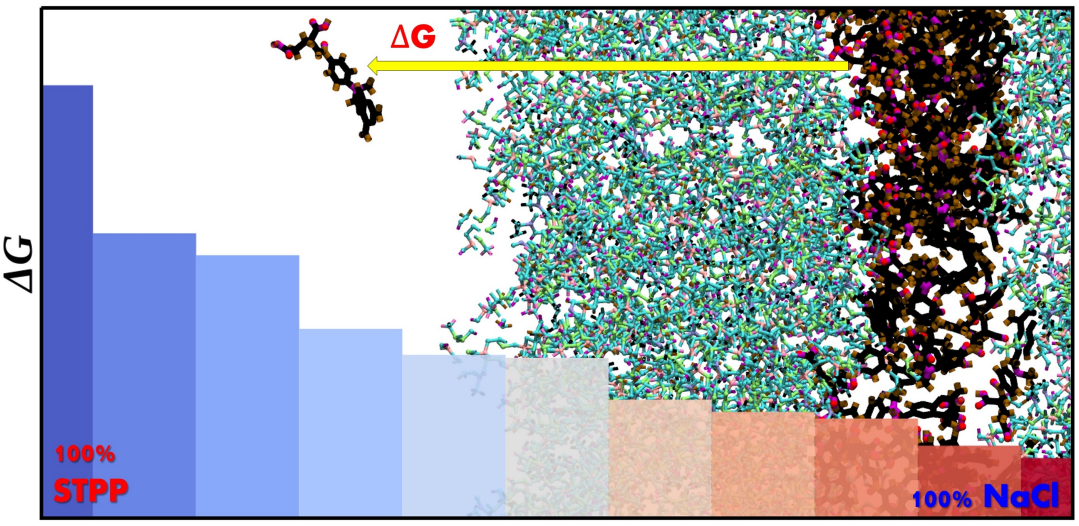

7.1 Introduction

Active and passive targeted drug delivery to treat various medical conditions has revolutionized medical practices, and the development of nanotechnology over the past few decades has provided a major thrust to it.[232] The effectiveness of therapy is associated with a drug's ability to specifically target and impact the biological functions of diseased cells while minimizing damage to healthy tissues. Nanoparticles (NP) and nanoassemblies, leveraging their unique characteristics, enable sustained and targeted drug delivery, thereby improving therapeutic outcomes.[233, 234] Development of nano-drug delivery systems for the controlled and targeted delivery of Methotrexate (MTX) included: a. polymeric NPs, which offer controlled and sustained drug release by diffusion through degradation and swelling of the polymer matrix;[235] b. lipid-polymer hybrid NPs, provide controlled release through a polymer core and enhanced stability and bioavailability

through a lipid shell;[236, 237] c. nanostructured lipid carriers – the presence of liquid lipids in the solid lipid matrix which enhances drug release properties,[238] d. solid lipid NPs; offer a stable release profile and protect the encapsulated drug from degradation,[239] and e. liposomes; enable controlled release through diffusion or fusion with target cell membranes[240, 241].

Chitosan (CS), a cationic polysaccharide, has a crystalline structure due to inter- and intramolecular hydrogen bonds. The presence of the N-acetyl group brings a degree of hydrophobic behaviour, though the main molecular chain is hydrophilic. Glycosidic linkage, a crucial structural element in glycans, plays a key role in determining their overall structure, functionality, and biological activities.[242–244] CS-based nanoformulation is nonhemolytic, biocompatible, and safe to utilize as a drug delivery mechanism. Hence, it could be an effective method for enhancing the therapeutic effectiveness of MTX toward solid tumours which is an anticancer and anti-inflammatory drug for treating various cancer and auto-immune diseases.[245] This drug inhibits dihydrofolate reductase, essential for producing tetrahydrofolates used in purine nucleotide synthesis, consequently hindering DNA synthesis and cellular replication.[246]

For drug delivery, polysaccharides are gaining attention due to their biocompatibility, biodegradability, and low immunogenicity. Reddy et al. showed how hydrophobic residues influence the binding of the drug molecules (act as an inhibitor) to $E.coli$ thymidylate synthase enzyme using the thermodynamic cycle perturbation approach.[247] Recently, Rana et al. investigated an MTX analogue with enhanced binding affinity, effectively inhibiting both wild-type and double-mutant human DHFR using molecular dynamics simulations for cancer therapeutics.[248]

STPP played a critical role as a cross-linker in reducing drug toxicity and enhancing targetability when MTX-loaded CS-NPs were covalently bonded with folic acid NPs, as developed by Ji et al. [249] MTX-encapsulated CS-NPs had higher cytotoxicity against prostate cancer cells compared to individuals due to improved cellular uptake and sustained release.[250] The more effective transdermal route allows continuous and con-

trolled drug delivery through the skin. MTX-loaded solid lipid nanoparticles showed an improved drug delivery in skin cancer therapy. Incorporated into a Carbopol 934 gel, the formulation showed excellent uptake in skin layers, superior pharmacokinetics, and enhanced efficacy.[251] Moreover, nanotechnology-based systems enable targeted drug delivery to specific cells or tissues, such as cancer cells, by exploiting unique features of the tumour environment or cell surface receptors.[252–254]

The development of drug delivery systems is crucial for personalized medicine, as it enables the creation of drugs designed to target an individual's genetic characteristics and disease traits.[255, 256] Al-Nemrawi et al. have investigated the transdermal delivery of MTX-loaded-CS-NPs for the treatment of rheumatoid arthritis.[257] Nogueira et al. investigated the effect of a bioactive surfactant with pH-sensitive properties on the anti-tumor activity and the intercellular behaviour of MTX-loaded-CS-NPs prepared by using a modified ionotropic complexation process. The pH-sensitive behaviour of NPs allowed the accelerated release in an acid environment, which facilitated the cytosolic delivery of endocytosed materials.[258]

Simulation studies offered a powerful means to optimize and design drug delivery systems by predicting the behaviour of drugs within the body through the release kinetics, and the interactions with biological tissues. Deepa et al. used the CS-NPs as a carrier for the controlled release of cytarabine in breast cancer cells using molecular dynamics simulation. They showed the encapsulation and release of single molecules of cytarabine from CS-based nano-formulation.[259] Similarly, as CS is one of the best polymers for encapsulating curcumin, Yadav et al. showed that CS-curcumin polymer complexes were formed through hydrogen bonds (binding energy of –4.3 kcal/mol) and exhibited in-vitro release of curcumin.[260] Sanaz et al. used the CS-based hydrogel as a sorbent synthesized by ionic gelation method for the micro-extraction from aqueous and plasma media.[261] Akolade et al. studied the encapsulation and release characteristics of curcumin loaded in CS-based drug delivery carriers, to find influencing parameters such as the ratio of curcumin to CS, crosslinking time, pH of CS solution and concentration of curcumin etc.[262] Dai et al. reported the translocation of MTX through a Carbon nan-

otube embedded in a lipid membrane as a function of electric field intensity. In addition, the Potential of Mean Force (PMF) provided the estimation of the change in free energy during the translocation process in different nanochannels.[263] Khnifira et al. have reported the adsorption mechanism of anionic dyes: tartrazine, sunset yellow, and brilliant blue on the CS (110) surface using molecular dynamics simulation. They showed that the three dyes are adsorbed in parallel on the CS (110) surface, and RDF analysis reveals that all the shortest intermolecular distances are less than 3.50 Å, suggesting the formation of a firmly adhered layer between the molecules and the CS (110) surface.[264] Pakdel et al. investigated the self-assembly and drug release in the presence of Camptothecin using all-atom molecular dynamics simulation and first-principles density functional theory calculations and showed that the combinations have a greater tendency to form a spherical-like structure than the free drug, which enhances the anticancer efficacy.[265] Bello et al. investigated the saturation capacity of the drug on PAMMAM-G4 dendrimer under saturated conditions across pH, employing Liquid-Driven Membrane Devices.[266] Mazloom-Jalali and Shariatinia investigated the polymeric nanocomposite of CS containing SiO_2 NPs designed for delivering the anticancer drug Pipobromane using molecular dynamics simulations.[267] Similarly, Amantea et al. reported the use of magnetic NPs coated with thermoresponsive polymers for controlled drug release in cancer treatment. The coated MNPs showed temperature-dependent release, with higher release at 43 °C than at 37 °C. The esterification of the copolymers altered the release rates and lowered the lower critical solution temperature, suggesting a tunable drug delivery system suitable for cancer treatment.[268] Recently, Ayyami et al. investigated the efficacy of MTX-functionalized-5-aminolevulinic acid-modified CS-based-manganese dioxide-NPs as targeted radiosensitizers for cancer treatment. The novel formulation aims to improve drug delivery and tumour targeting while ensuring biosafety. Detailed mechanistic insights on how these NPs interact at the molecular level with cancer cells under radio sensitization are still needed to fully understand the pathways involved in cell death.[269]

Building upon our understanding of micelle-mediated nucleation, we extended our investigation to the field of controlled drug delivery. While the previous study focused on

the nucleation and growth of gold nanocrystals facilitated by micellar environments, here we explore how polymeric matrices, such as chitosan cross-linked with STPP, can similarly regulate the release dynamics of encapsulated drug molecules. By applying similar molecular dynamics simulation techniques and free energy landscape analysis, we aim to elucidate the fundamental mechanisms governing drug release, paralleling the transport and energetic barriers observed during nanoparticle nucleation processes.

In this study, we investigated a CS-based drug delivery carrier. The CS chains were ionically cross-linked by STPP to form a highly rigid CS matrix, which was loaded with MTX. The current work evaluated the performance of CS NPs as a carrier for the controlled release using molecular dynamics simulation by estimating the free energy for the release. It will provide detailed insights into the interaction with the solvent, offering a microscopic view of the energy landscape. We have quantified the effect of STPP concentration on the release behaviour of the drug into the aqueous solution of ethanol.

7.2 Models and Methodology

In this work, a CS matrix was used as the carrier for the MTX drug.[270] The initial configuration of MTX in the CS-STPP matrix was generated by placing 50 molecules inside the matrix. The matrix consisted of 98 CS chains with 10 repeating units and 98 molecules of STPP. The structure of CS (PMCID: PMC5870669)[271] was generated using Glycan Reader and Modeller as available in CHARMM-GUI.[272] The structure of MTX (PDB ID:3QXT)[273] and STPP (PDB ID:5A60)[274] were taken from the RCSB protein data bank. [275] Chemical structures of complex molecules - chitosan, STPP, and MTX, are shown in Figure 7.1. CHARMMS36 forcefield[94] was used to model bonded and non-bonded interactions for non-solvent molecules, and the TIP3P model[95] was used for water molecules as the solvent.

Further, the CS-STPP-MTX assembly was placed at the centre of the simulation box with dimensions of $23.5 \times 6.9 \times 6.9$ nm^3. The box was filled with water molecules. Na^+ and Cl^- ions were added to neutralize the system. The energy of the solvated system

was minimized using the steepest descent method. During the simulation, the temperature and pressure were maintained at 303.15 K and 1 atmosphere, respectively, using the Nosé-Hoover thermostat (relaxation time is 0.5 ps)[212] and Parrinello-Rehman barostat (relaxation time is 1.0 ps).[105] The van der Waals interactions were modelled per Lennard-Jones with a cut-off of 1.0 nm. Long-range electrostatic interactions were calculated using the particle-particle particle-mesh (PPPM) method [98] with a real space cut-off of 1 nm, a grid spacing of 0.8 nm, and an interpolation order of 10^{-4}. Bonds and angles were constrained using the SHAKE algorithm.[100]

All the systems were equilibrated in the NVT ensemble for five ns after energy minimization. After equilibration, the systems were allowed to evolve for 50 ns in the NPT ensemble with a timestep of 2 fs to integrate the equation of motion using the Velocity Verlet algorithm[89] and the coordinates of the constituent atoms were stored every 10 ps for the calculation of properties and visualization. Molecular dynamics simulations were carried out using LAMMPS[211], and VMD[150] was used to visualize the simulation trajectories. The change in free energy for the MTX during its voyage from inside the CS matrix to the outside solvent was calculated using umbrella sampling.[155]. We used the Weighted Histogram Analysis Method (WHAM)[154] to remove the biasing potential and reconstruct the potential of mean force (PMF) between the encapsulated one and the solvated one. In this case, 32 windows with 2Å spacing along the reaction coordinate were used for biased MD simulations. We selected the centre of mass of a single molecule, randomly inside the matrix which was tethered linearly along the x-direction till it reached a distance far from the matrix inside the bulk solvent. We performed a 1.0 ns run for each window (as the polymer matrix was highly cross-linked) at 303.15 K with restraints using a harmonic force constant of 100 kcal/mol. $Å^2$. While constructing PMF using WHAM, the number of bins was set to 100 with a tolerance for iterations of 10^{-5}. For all the simulations, the temperature was maintained at 303.15 K.

To investigate the effect of cosolvent and salts on the release, we added ethanol and NaCl to the system. To quantify the effect of the cross-linking agent, STPP, we randomly replaced the anion TPP with chloride ions. The concentration of ethanol and NaCl in water is

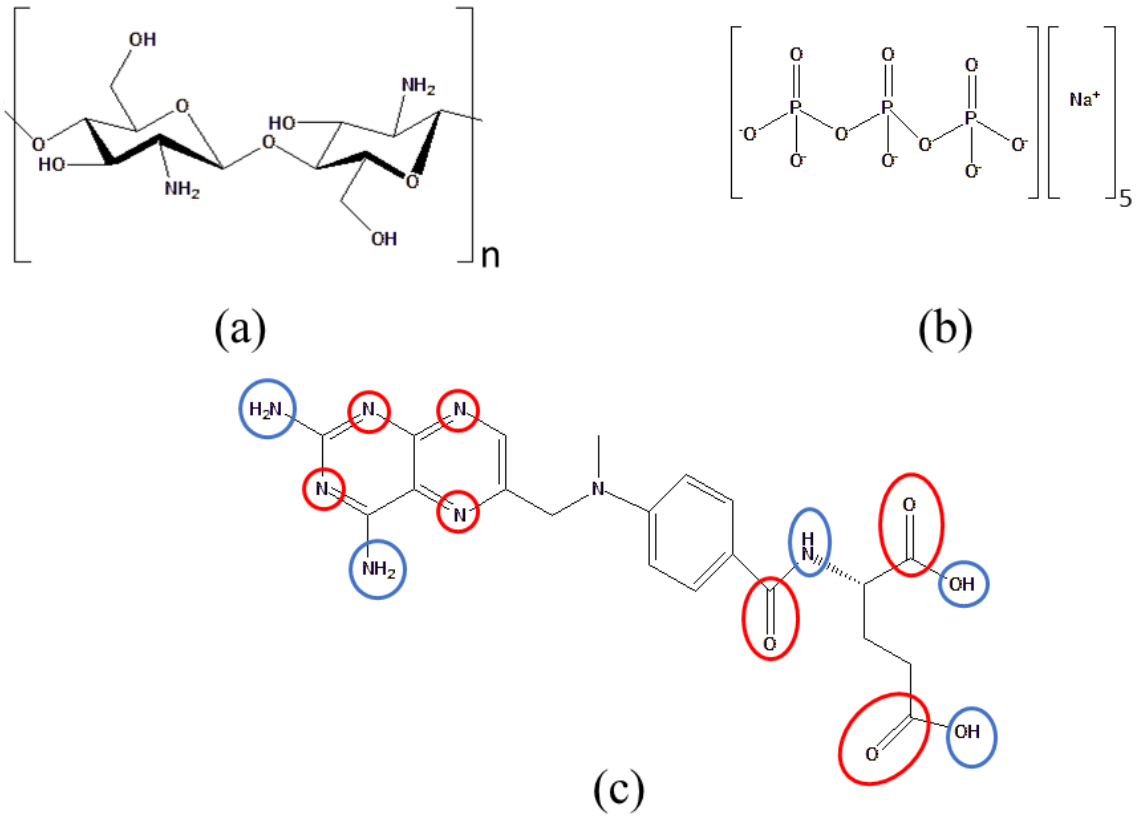

Figure 7.1: Chemical structure of (a) Chitosan, (b) STPP, and (c) Methotrexate molecule. Blue and Red circles indicated the hydrogen bond donor and acceptor sites respectively.

29.43 g/l (0.639 M) and 149.38 g/l (2.56 M). We have used CHARMMS36 forcefield for ethanol as well.[94]

7.3 Result and Discussion

We started the discussion by encapsulating MTX molecules inside the CS polymer matrix that are cross-linked with STPP. Here, we have calculated the structural arrangement of MTX inside the CS matrix in an aqueous solution, such as the density profile and radial distribution function. In particular, we calculated mass densities of MTX, STPP, CS, and water to quantify the encapsulation of MTX inside the CS-STPP polymer matrix.

Figure 7.2(a) depicted a snapshot of the system at the end of the production run. The greenish matrix represents the arrangement of CS-STPP within the simulation box, while the MTX drug molecules are depicted as brown-red beads. These drug molecules are well-

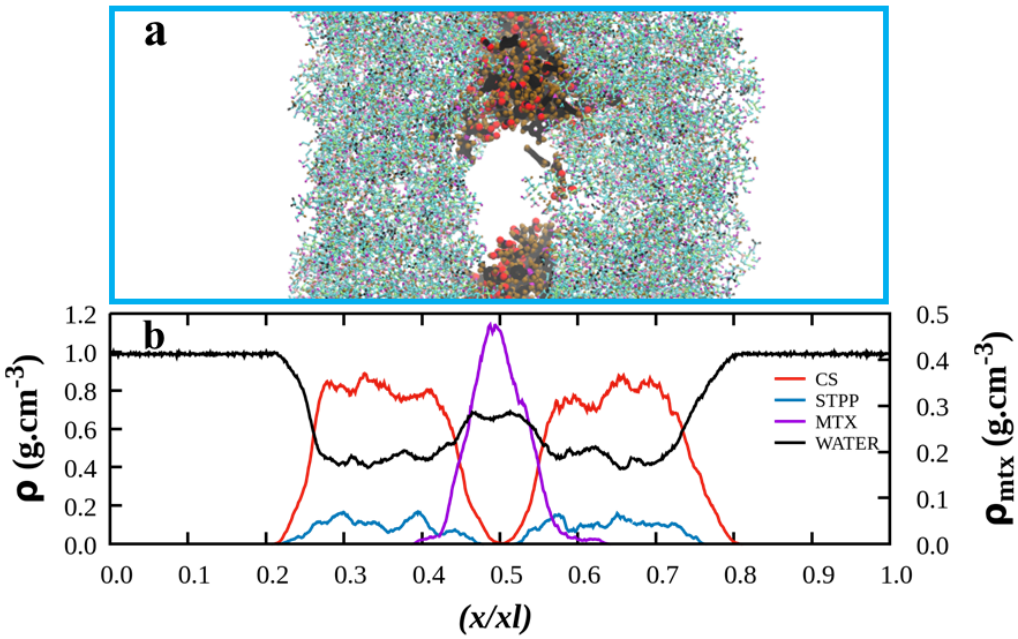

Figure 7.2: (a) Snapshot of the system at the end of production run (50 ns); the blue box represents the simulation box filled with water; the CS - STPP were presented as a greenish bonded structure, and the MTX molecules were shown in red and brown bonded spheres. Water molecules were omitted here for clarity. (b) The density profiles of CS, STPP, MTX, and water were shown in respective colors against the reduced length of the simulation box.

encapsulated within the CS matrix. Although the system was dissolved in water, the water molecules are omitted for clarity. The overall density of the system was determined to be 1.17 ± 0.01 g.cm^{-3}. Interestingly, the MTX molecules demonstrated self-aggregation within a pocket of the CS matrix. Figure 7.2(b) represented the density profiles of the different components, depicted in distinct colors. These profiles were generated by analyzing the densities across vertical slabs with a thickness of 0.2 nm throughout the simulation box. The data revealed that the CS-STPP-MTX complex was thoroughly solvated, with a noticeable decrease in water density attributed to the presence of this moiety. The density profile of the drugs, represented by the purple line and scaled on the right-hand axis, indicates that the encapsulated MTX molecules created voids for water molecules, leading to a localized increase in water density near the centre of the simulation box. The CS density profile exhibited symmetry about the midpoint of the simulation box, while the STPP profile also mirrored this symmetry, aligning closely with the CS distribution.

Figure 7.3 provided detailed insights into the structural organization of the CS matrix and

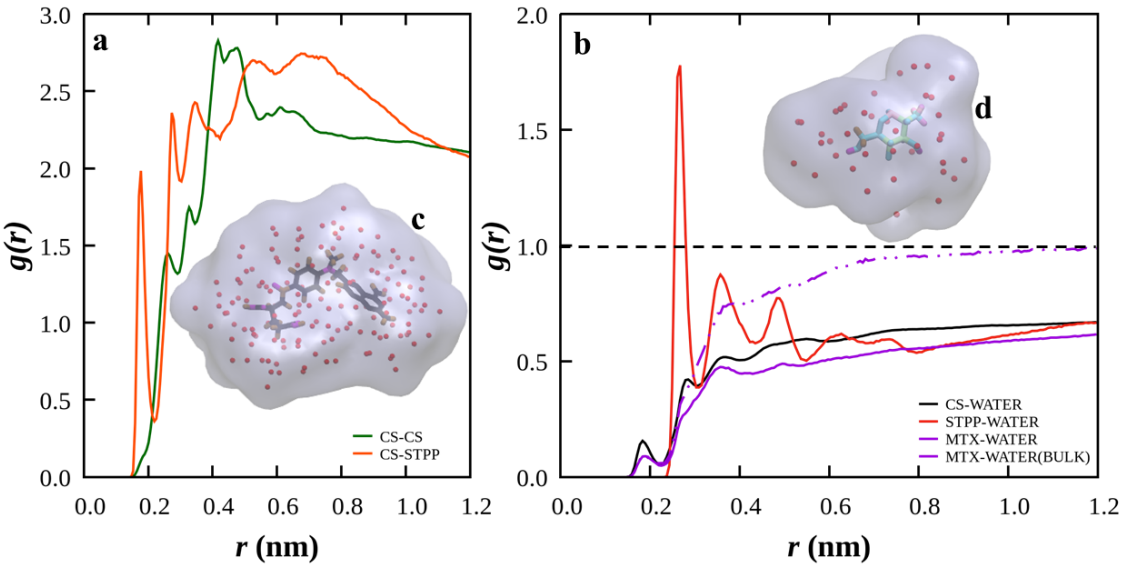

Figure 7.3: The radial distribution for (a) CS-CS and CS-STPP pairs, (b) different components of the solutions with water (i.e. CS-WATER, STPP-WATER, and MTX-WATER). A dashed purple line is used to represent the RDF for the MTX-WATER pair in an aqueous solution. In Figures c and d, isosurface representations of the solvation shell of the MTX drug and CS monomer, respectively. Molecules are shown using bonded structures, and Oxygen atoms of water molecules are shown using red spheres.

its interaction with water molecules, as well as the relative arrangement of STPP and MTX molecules, through radial distribution function (RDF) analysis. In Figure 7.3(a), the RDF of CS monomers exhibits a broad peak at approximately 0.4 nm (green line), indicative of the flexible and amorphous nature of the CS matrix. Notably, the polymer matrix lacks periodicity along the x-dimension. The RDF profile for the CS-STPP pair shows a sharp peak at $\sim$ 0.18 nm, suggesting strong and specific interactions between CS and STPP. These interactions are likely due to hydrogen bonding or ionic interactions between the functional groups of the CS chains and the phosphate groups of STPP, which acts as a cross-linking agent, imparting structural rigidity to the matrix. The structural arrangement of water molecules relative to the system components is presented in Figure 7.3b. The RDF of water molecules around STPP (red line) shows a sharp peak at $\sim$ 0.267 nm, reflecting a well-defined solvation shell around STPP. This strong solvation shell, absent for the other components, arises from pronounced electrostatic interactions between water molecules and STPP. Additionally, STPP's strong bonding with CS (as observed in Figure 7.3(a)) results in its uniform dispersion within the CS matrix, limiting the number of water

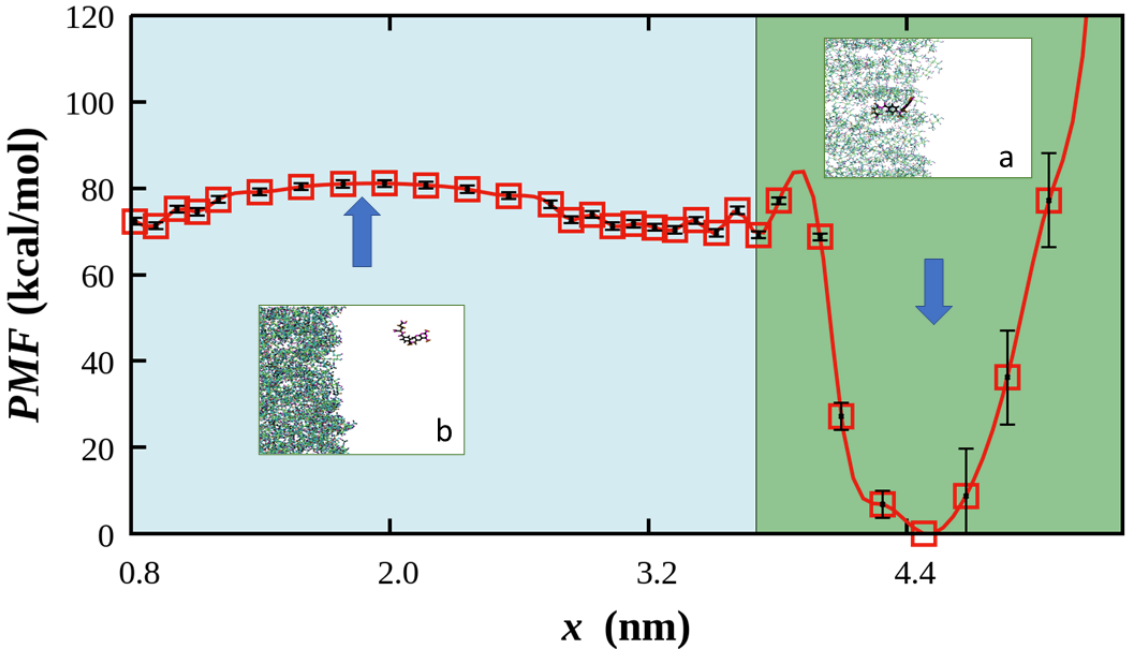

Figure 7.4: Free energy landscape of the release of MTX into the water. The x-axis indicates the reaction coordinate in the reduced unit. The Cyan and green zones represent water and a CS-STPP matrix, respectively. Insets a and b show the snapshot of the binding of MTX with the CS-STPP matrix and an MTX molecule in water.

molecules that can surround an individual STPP molecule. Consequently, the RDFs for the system components do not converge to unity within the cutoff distance. The RDF for the water-CS pair exhibits a small peak at ~ 0.189 nm, indicating a weaker interaction between water and the CS polymer. This interaction is facilitated by the hydroxyl groups of CS, which act as hydrogen-bonding sites. The water-MTX RDF (purple solid line in Figure 7.3(b)) shows a trend similar to the water-CS interaction, with the RDF gradually approaching the bulk density. This suggests weaker interactions between MTX and water compared to MTX in bulk water (shown by the purple dashed line). Moreover, as observed in Figure 7.2(a), the MTX molecules aggregate within the CS matrix, limiting their exposure to water in all directions. Figures 7.3(c) and 7.3(d) depicted the solvation layers of MTX and a CS monomer, respectively, up to a distance of 0.6 nm. Due to their larger size, MTX molecules have a greater solvation shell volume compared to CS monomers. However, MTX exhibits a relatively low affinity for water, as evidenced by the RDF profile with bulk water. To further understand the release mechanism of MTX from the CS matrix, it is essential to estimate the associated free energy of the process.

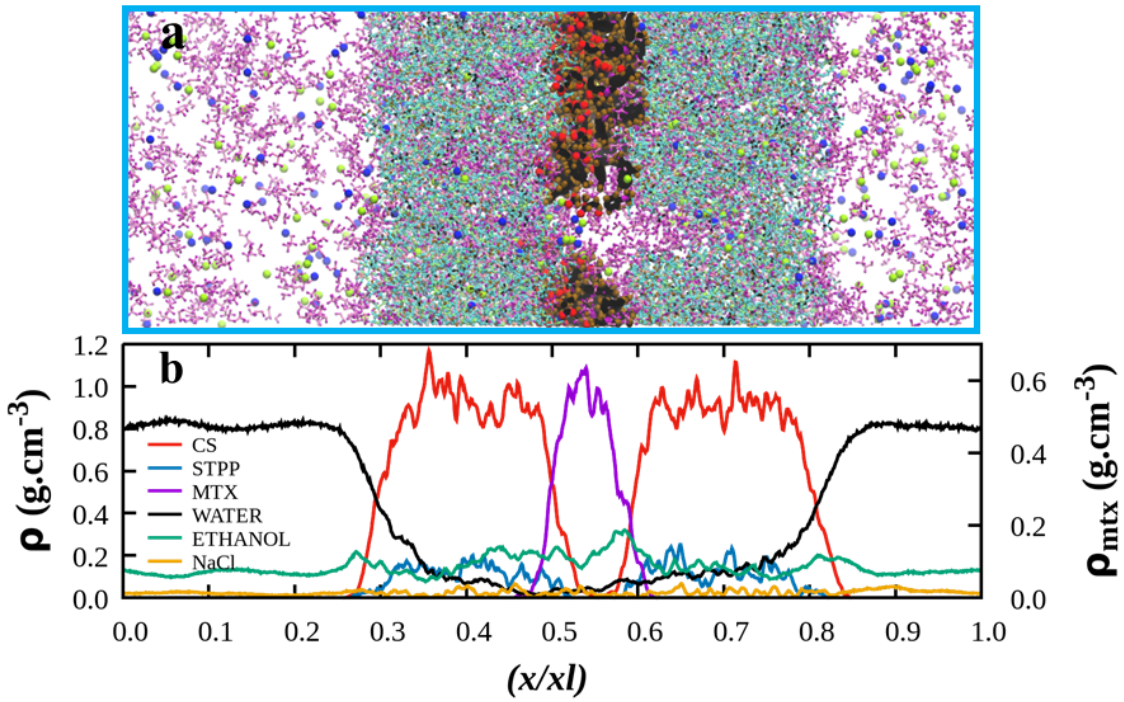

Figure 7.5: (a) Snapshot of the system at the end of the production run (50 ns). The simulation box filled with water is represented by the blue line; the MTX molecules were displayed as red and brown bonded spheres, and the CS - STPP were presented as a greenish bonded structure. The molecules of ethanol were shown as being pink in color. The colors of the Na^+ and Cl^- ions were displayed as blue and light green, respectively. For clarity, water molecules were omitted here. (b) The density profiles of CS, STPP, MTX, ETHANOL, NaCl and water were shown with respective colors along the reduced length of the simulation box.

Figure 7.4 depicts the free energy landscape for the release of MTX from the CS-STPP matrix into water. The results indicate that MTX adopts a more stable conformation within the CS-STPP matrix, as evidenced by lower Gibbs free energy values. Conversely, in the aqueous environment, MTX exhibits a higher Gibbs free energy, reflecting an energetically less favorable state. Insets (a) and (b) illustrate the binding of MTX within the CS-STPP matrix and its solvated state in water, respectively. The free energy required for the release process was calculated to be ~ 81.123 kcal/mol. This substantial energy barrier underscores the thermodynamic stability of MTX within the CS matrix and highlights the significant challenge in facilitating its efficient release. To mitigate this barrier and enhance the release efficiency, ethanol was introduced as a co-solvent, offering a potential strategy to reduce the energy requirement for the release process.

Figure 7.5(a) presents a snapshot of the system at the conclusion of the production run.

The arrangement of CS-STPP within the simulation box is depicted as a greenish matrix, while the MTX molecules are represented by brown-red beads. The MTX molecules are observed to be well-contained within the CS matrix. As in Figure 7.2(a), the system is dissolved in a solvent; however, water molecules are omitted in the visualization for clarity. In contrast to Figure 7.2(a), the MTX molecules appear more dispersed in the presence of ethanol, which is shown as pink beads. Additionally, the CS matrix exhibits noticeable swelling due to the incorporation of ethanol molecules into its structure. The density profiles of the individual components—CS, STPP, MTX, and water—are shown in Figure 7.5(b). The MTX molecules remain closely associated and encapsulated by the CS-STPP matrix. The density profile of ethanol (green line) indicates that ethanol molecules are well-dispersed within the water phase and accumulate in higher concentrations near the MTX-aggregated regions. This behavior can be attributed to the intercalation of ethanol molecules among the stacked MTX molecules. Notably, the water density peak observed in Figure 7.2(b) is absent in this case, consistent with the increased dispersity of MTX molecules within the matrix. The incorporation of ethanol molecules disrupts the dense water solvation layer, leading to the redistribution of molecular arrangements within the CS-STPP matrix. Ethanol molecules preferentially aggregate in the vicinity of MTX clusters, resulting in the depletion of water density in those zones, as illustrated in Figure 7.5(b). This analysis highlights the structural modifications induced by ethanol and provides insights into the interaction of ethanol with MTX and the CS-STPP matrix, which could have implications for optimizing drug release mechanisms.

Figure 7.6(a) depicts the radial distribution function (RDF) for CS-CS and CS-STPP pairs in water and aqueous ethanol. A broad peak at ~ 0.4 nm is observed for both environments, indicating the amorphous nature of the CS moiety, which is preserved in water as well as aqueous ethanol. However, the peak height decreases in the presence of ethanol, suggesting that ethanol molecules are infused into the CS matrix. Conversely, for the CS-STPP pair, the inclusion of ethanol leads to a rise in the peak position, indicating stronger interactions between STPP ions and CS units. This behavior is likely a result of ethanol molecules intercalating within the CS moiety, which enhances the attachment of

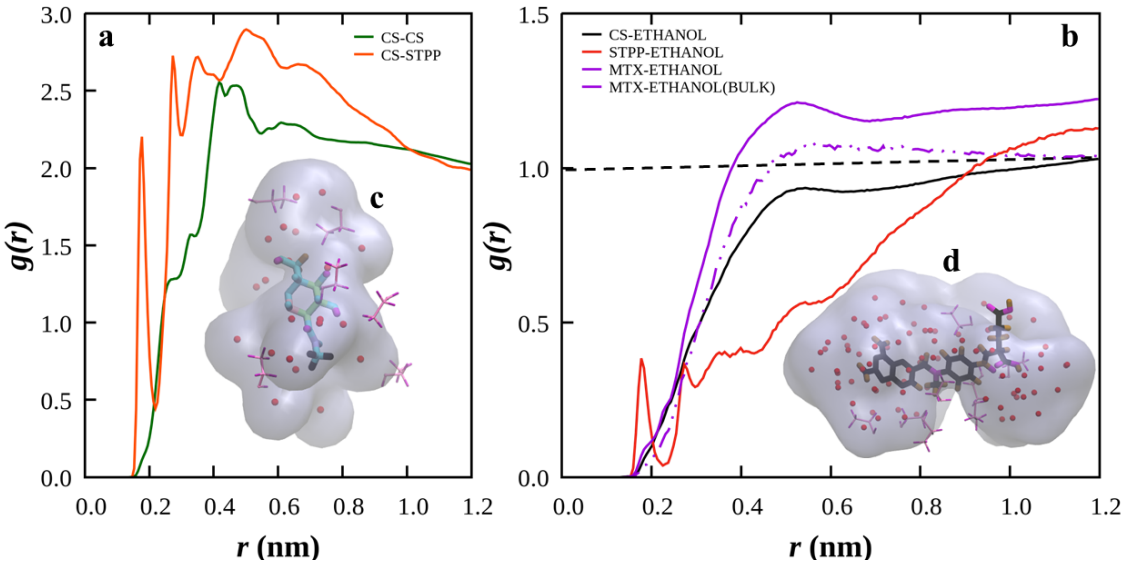

Figure 7.6: (a) The radial distribution function for CS-CS and CS-STPP in water and aqueous ethanol solution. Solid and dashed lines are used for the RDF in water and aqueous ethanol solution, respectively. (b) The radial distribution function between ethanol molecules and CS, STPP, and MTX pairs at 303 K is represented by black, red, and purple lines, respectively. A dashed purple line indicates the radial distribution of ethanol molecules around MTX molecules in an aqueous solution of ethanol.

STPP to CS chains. Nevertheless, the overall structural rigidity of the matrix is reduced due to the incorporation of ethanol. Figure 7.6(b) presents the RDF of ethanol molecules around CS units, STPP, and MTX molecules at 303 K. The RDF for STPP-ethanol interactions (red line) exhibits a peak at ~ 0.177nm, signifying weak binding between STPP and ethanol. Ethanol molecules do not form a localized solvation shell around STPP, as the local density remains consistently lower than the bulk density. In contrast, the RDF for CS-ethanol and MTX-ethanol pairs do not display sharp peaks or well-defined structural arrangements. However, ethanol demonstrates a higher affinity for CS and MTX compared to water, suggesting that ethanol is a more favorable solvent for the system. Ethanol molecules form a stronger solvation shell around MTX within the matrix (solid purple line) than in pure ethanol (dashed purple line). This enhanced interaction between ethanol and MTX is indicative of significant interplay between water and ethanol, altering the dynamics within the matrix. These changes in molecular dynamics are expected to influence the drug release process. To quantify the effect of ethanol on the release dynamics, the free energy required for MTX release from the CS-STPP matrix must be calculated. This would provide a comprehensive understanding of the role of ethanol in modifying

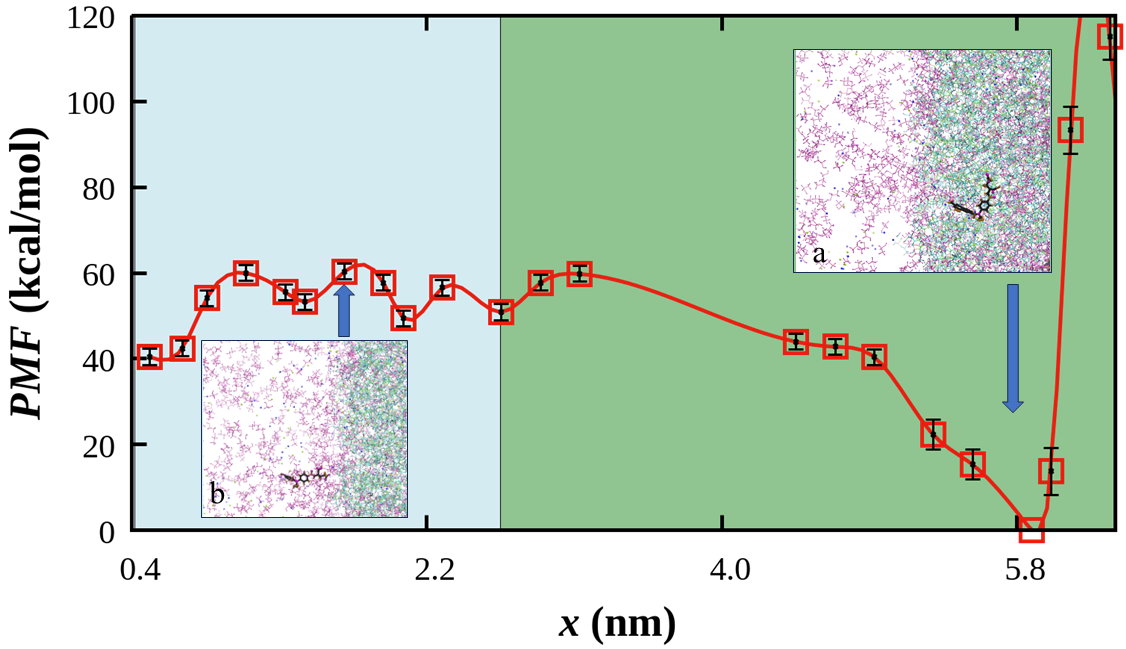

Figure 7.7: Free energy landscape of the release of MTX into the ethanol-water solution. The x-axis indicates the reaction coordinate in nm. The Cyan and green zones represent water and a CS-STPP matrix, respectively. Insets a and b show the snapshot of the binding of MTX with the CS-STPP matrix and an MTX molecule in an ethanol-water solution.

the release process.

Figure 7.7 shows the free energy landscape for the release of MTX into an aqueous ethanol solution. The free energy required for the release process was reduced to 52.4 kcal/mol compared to the energy required in a purely aqueous environment. This reduction can be attributed to the hydrophobic effects of ethanol, which, being less polar than water, accommodates the hydrophobic regions of the MTX molecule more effectively. This minimizes the energy barrier associated with introducing hydrophobic moieties into a polar environment, resulting in a lower overall free energy. The interaction between MTX and the ethanol-water mixture is likely to be enthalpically more favorable, with the increased disorder in the mixed solvent system further contributing to the reduction in free energy. While water forms extensive hydrogen-bonding networks, the inclusion of ethanol disrupts these networks to some extent.[276] Such disruption decreases the stabilization energy provided by hydrogen bonding in water, resulting in a less steep free energy landscape.[277] To further reduce the free energy barrier, weaker cross-linkers were introduced in place of STPP. The effects of this modification on the free energy landscape and the

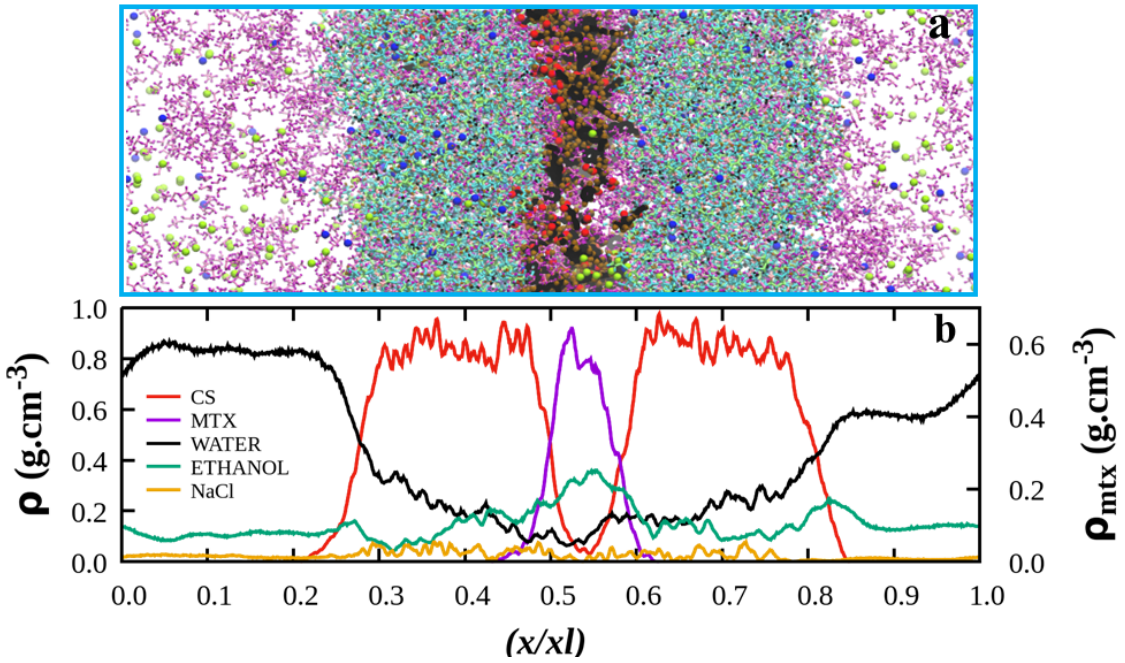

Figure 7.8: (a) Snapshot of the system after the production run where CS was represented as the green bond structure, MTX molecules were shown in red and brown bonded spheres, and ethanol molecules were represented as pink bonds, Na+ and Cl- ions are shown as blue and light green spheres, respectively. The blue line represents the simulation box filled with water molecules, indicating the boundaries of the simulation environment. This system does not contain STPP molecules. Water molecules were omitted for clarity. (b) The density profiles of CS, MTX, ethanol, NaCl and water were shown with respective colors along the reduced length of the simulation box.

MTX release process are discussed in subsequent sections.

Figure 7.8(a) depicts a snapshot of the system taken after a 50 ns production run. The greenish matrix represents the configuration of the CS polymer within the simulation box, while the brown-red beads depict the encapsulated methotrexate (MTX) molecules within the CS matrix. The entire system is solvated in water; however, water molecules are omitted from the visualization for clarity. In this configuration, the STPP molecules were replaced with an equivalent number of smaller anions to evaluate their impact on the system. Figure 7.8(b) shows the density profiles of the individual components, including water, CS, ethanol, NaCl, and MTX. The CS matrix exhibited swelling in the ethanol-water mixture, as evidenced by the broader density profile (red line) compared to the profile observed in Figure 7.2(a). This swelling is more pronounced than the CS density profile in Figure 7.5(b), highlighting the structural modifications induced by the solvent and the removal of STPP. The ethanol density profile (green line) reveals a broad peak within the

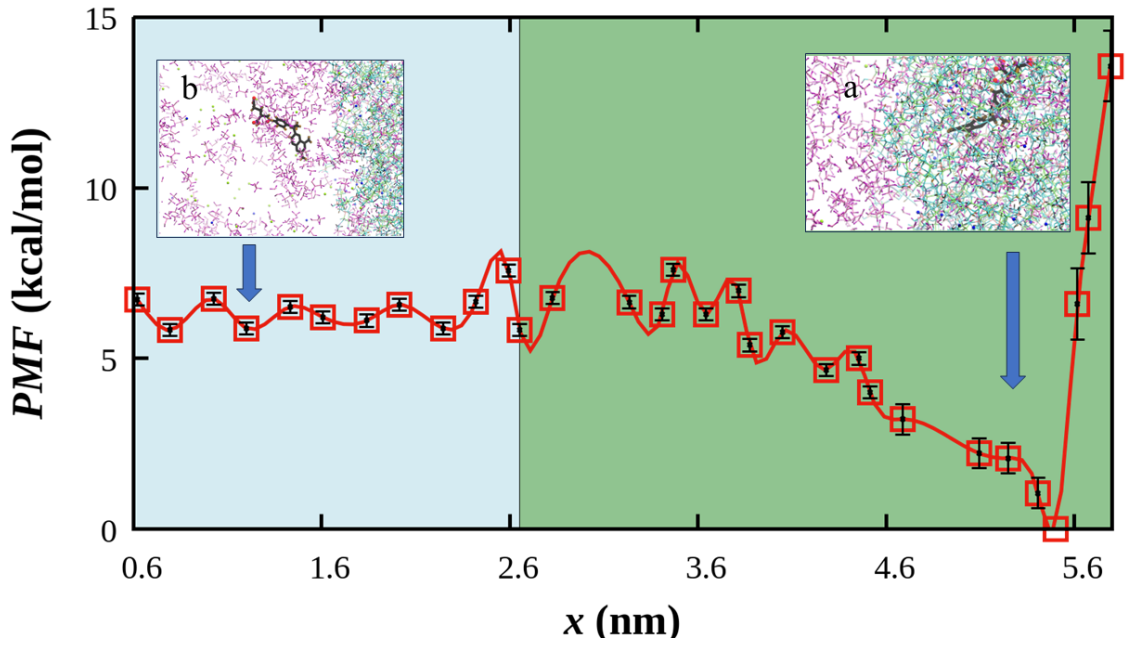

Figure 7.9: Free energy landscape of the release of MTX into the ethanol-water solution in the absence of cross-linker STPP. The x-axis indicates the reaction coordinate in nm. The Cyan and green zones represent water and a CS matrix, respectively. Insets a and b show the snapshot of the binding of MTX with the CS matrix and an MTX molecule in an ethanol-water solution.

MTX zone, where water concentration is notably depleted. This behavior indicates that ethanol plays a significant role in altering the solvation environment of both CS and MTX. The MTX density profile shows a strong and broader peak, reflecting enhanced solvation and interaction with ethanol in the absence of the cross-linking STPP molecules. The inclusion of smaller anions in place of STPP reduced the degree of cross-linking within the CS matrix. This reduction in cross-linking has implications for the structural stability and dynamics of the system, which warrants further investigation. Quantifying the impact of this modification in terms of free energy will provide deeper insights into its effects on the MTX release mechanism.

Figure 7.9 shows the free energy landscape for the release of MTX into an aqueous ethanol solution in the absence of STPP cross-linkers. The calculated free energy for the release process was significantly reduced to 5.833 kcal/mol, compared to 81.1 kcal/mol observed in the presence of STPP (as shown in Figure 7.4). This substantial decrease in free energy indicates a more favorable environment for the solubilization of MTX when the cross-linker STPP is absent. The strong ionic interactions between multivalent STPP molecules

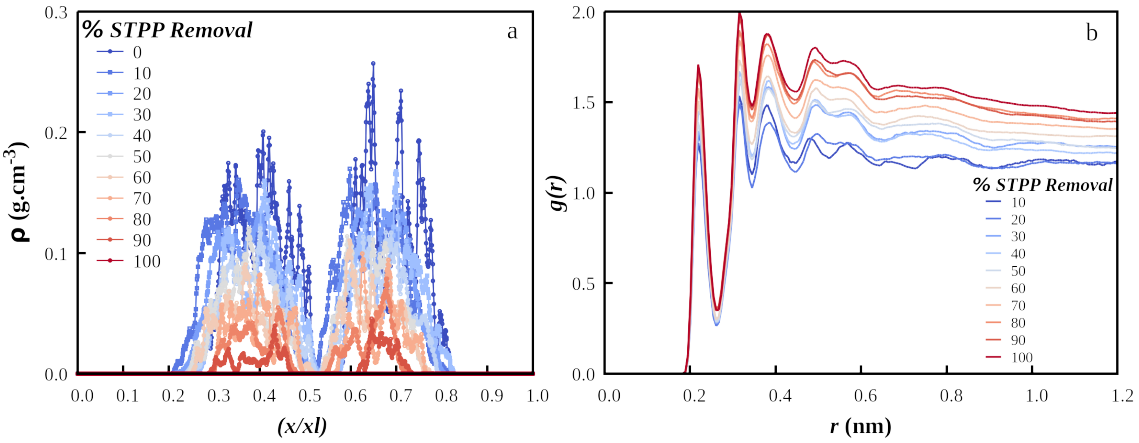

Figure 7.10: (a) Density profile of STPP along the reduced length of the simulation box, blue to red color gradient shown the density profile of STPP as TPP replaced with an equivalent number of chloride ions, (b) Radial distribution function of chloride ions – CS pairs as removal of TPP from 0 to 100 %, blue to red color gradient represents the RDF profiles of chloride ions – CS pairs at the different extent of chloride ions.

and CS units, as seen in the previous configuration, result in a highly stable CS-STPP complex that requires higher energy to release MTX, as depicted in Figure 7.4. The replacement of STPP molecules with smaller anions weakens these interactions, thereby reducing the cross-linking density within the CS matrix. This leads to a less rigid polymer structure and facilitates the release of MTX into the solution, as evidenced by the lower free energy requirement. The absence of STPP cross-linkers thus significantly alters the structural and thermodynamic properties of the CS matrix, enhancing the potential for MTX release under these modified conditions.

Delving into the structural organisation of anions in the CS matrix, we looked into the density profiles and radial distribution functions. Figure 7.10(a) shows the density profiles of the anions. The anions, TPP ions, were randomly replaced with the equivalent number of chloride ions, so it should be ensured that the removal of the molecules is carried out uniformly. The uniformly random removal of the STPP molecules also ensured that the chloride ions were uniformly distributed inside the CS chains and held the matrix together. It is required to estimate where the chloride ions are getting bound. For that, we have calculated the radial distribution functions between the CS matrix and chloride ions at the different concentrations of chloride ions. Figure 7.10(b) shows the radial distribution function of chloride ions with CS monomers as a replacement for TPP. The first peak

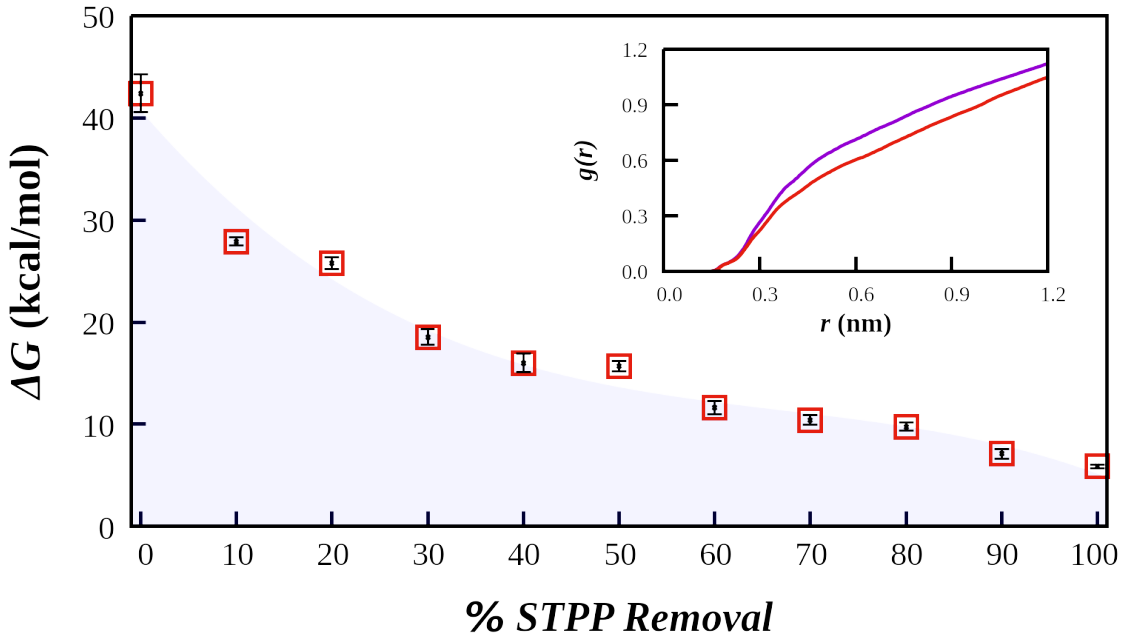

Figure 7.11: Change in free energy for the release of MTX molecules at different fractions of STPP, the cross-linker of CS, was replaced by NaCl. The inset shows the change in the CS-MTX pair correlation function in the presence (purple line) and absence (red line) of STPP in the solution.

at $\sim$ 0.22 nm, indicates that chloride ions are strongly bound to the CS polymer. As the concentration of chloride ions increases, the coordination number of the chloride ions near a CS monomer increases, indicated by an increase in the peak height. The second peak, at 0.35 nm, also gradually increases with increasing concentration of the chloride ions. The RDF showed an oscillating nature and gradually approached unity. The nature of RDF indicated that the ions and CS monomers were strongly correlated.

Figure 7.11 depicts the free energy change associated with the release of MTX from the CS polymer into an ethanol-water solution as a function of the percentage of STPP. The results show that the free energy required for drug release decreases progressively with the gradual removal of STPP, from 100 % to 0 %. This trend indicates that as the concentration of STPP decreases, the release process becomes energetically more favorable, requiring less energy. The reduction in free energy is attributed to increased interactions between the CS polymer and chloride ions, which disrupt the stronger interactions between CS and MTX. The inset in Figure 7.10 shows the radial distribution function (RDF) between CS and MTX. In the presence of STPP, the pair correlation between CS and MTX is stronger,

indicating a more stable interaction. However, with the removal of STPP and its replacement by chloride ions, the pair correlation weakens. This suggests that the inclusion of chloride ions disrupts the CS-MTX interaction, thereby facilitating the release of MTX with significantly lower energy requirements. In an ethanol-water solution, chloride ions play a critical role in the solvation process. As STPP is replaced by chloride ions, the CS polymer interacts more freely with these ions. This interaction enhances the solvation of the CS polymer, reducing its affinity for MTX molecules. Consequently, the solvation process promotes the diffusion of MTX out of the polymer matrix and into the ethanol-water solution, making the release process energetically more favorable. These findings highlight the importance of cross-linker concentration and ion composition in optimizing the release dynamics of encapsulated drugs.

7.4 Summary

In this work, the release of an encapsulated MTX within the CS-STPP matrix has been studied to understand the release of the drug using molecular dynamics simulations. A thorough analysis of the potential of mean force, calculated using advanced sampling techniques – Umbrella Sampling and WHAM analysis- indicated the energetic feasibility of releasing the drug into the aqueous solution from a CS-STPP matrix. This estimation of free energy will help us to develop a more sustainable and controllable drug release process. Our results indicated that the magnitude of energy required to release the drug into the water was more significant than that in the presence of ethanol and salts. Different degrees of cross-linking or different concentrations of cross-linking agents reduce the energy barrier, and the drug is easily released into the solution.